13th World Conference on Earthquake Engineering
Vancouver, B.C., Canada
August 1-6, 2004
Paper No. 8

A SUBSYSTEMS METHOD IN SIMULATION OF EARTHQUAKE GROUND MOTIONS USING A DIRECT 3-D BOUNDARY ELEMENT METHOD

Takanori HARADA[1], Yousuke OKADA[2], Koutaku OHO[2], and Masaki KOBAYASHI[3]

SUMMARY

Since the physical processes of propagation of seismic waves generated by a kinematic model of fault rupture in laterally inhomogeneous layered media can be consistently and rigorously represented by the boundary integral equations and these equations can be numerically solved with making use of the direct boundary element method, the simulation method of ground motions using the 3 dimensional BEM is attractive from a theoretical viewpoint. In this paper, to improve the weak points of the 3 dimensional BEM concerning the capacity of computational memory and the computational time, the method of subsystems analysis of entire system consisting of an earthquake source and the laterally inhomogeneous layered media has been developed. The advantages of the developed method of subsystems analysis have been demonstrated by the numerical examples of simulation of ground motions for an earthquake source and sedimentary valley model.

INTRODUCTION

Because the physical processes of propagation of seismic waves radiated from an earthquake source (kinematic model of fault rupture) in the laterally inhomogeneous layered media can be consistently and rigorously represented by the boundary integral equations or the elastodynamic representation theorem, for example, Pao and Varatharajulu [1], Aki and Richards [2], which can be numerically solved with making use of the direct boundary element method, for example, Manolis and Beskos [3], the simulation of earthquake ground motions based on the direct boundary element method is attractive from a theoretical point of view. However, it has disadvantage from a numerical point of view, since it requires the big capacity of computational memory and the computational time when it is used in the engineering simulation of earthquake ground motions up to high frequency range for the entire system consisting of an earthquake source and the laterally inhomogeneous layered media.

[1] Professor, Dept. of Civil and Environmental Engineering, Miyazaki University, Japan, Email:harada@civil.miyazaki-u.ac.jp
[2] Graduate Students, Dept. of Civil and Environmental Engineering, Miyazaki University, Japan
[3] Engineer, MAEDA CORPORATION, Japan

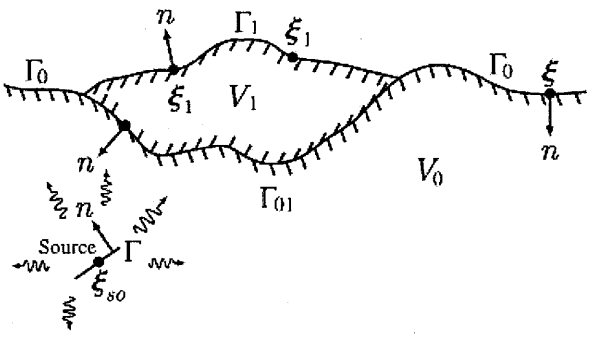

Figure 1 Seismic source and laterally inhomogeneous layered media and their notations

In order to improve the above numerical disadvantage, in this paper, the method of subsystems analysis has been proposed for the simulation of ground motions using a direct 3 dimensional boundary element method. The advantages of the developed method of subsystems analysis have been demonstrated by the numerical examples of simulation of ground motions of a single laterally inhomogeneous valley due to a strike slip fault rupture, indicating the drastic reduction of requiring capacity of computer memory and the computational time.

Although the proposed method of subsystems analysis in this paper is explained by using the direct boundary element method, respecting the theoretical consistency of the boundary integral representation of the seismic source and seismic wave propagation in the laterally inhomogeneous layered media, the concept of this method can be applied to the other numerical methods, the finite element method, the finite difference method, etc., and to the combined methods of these numerical methods.

FORMULATION OF ENTIRE SYSTEM ANALYSIS USING BEM

We start from a brief review of the formulation of analysis of the entire system, consisting of an earthquake source and the laterally inhomogeneous layered media as shown in Fig. 1, using the boundary element method (BEM). In Fig.1, V_0 indicate the half space region including an earthquake source represented by the kinematic model of faulting process, and V_1 the sedimentary surface layer. Also, Γ_0, Γ_1 are the free surfaces of the two regions V_0, V_1, respectively, and Γ_{01} the interface boundary between the two regions V_0 and V_1. In Fig.1, the unit normal vector and the positioning vector on the surface of the boundary of the regions are denoted by $\mathbf{n}$ and ξ, although they are not explicitly appearing in the following formulations because the boundary integral formulations of the system as shown in Fig. 1 are omitted for simplicity.

Now, using the boundary integral formulation of the exterior problem of elastodynamics in the frequency domain (Pao and Varatharajulu [1]) and its discretization on the basis of the boundary element method (BEM, for example, Manolis and Beskos [3]), we can obtain the matrix form of the boundary integral equation for the region V_0 such as,

$$\begin{bmatrix} \boldsymbol{H}_{11}^0 & \boldsymbol{H}_{12}^0 \\ \boldsymbol{H}_{21}^0 & \boldsymbol{H}_{22}^0 \end{bmatrix} \begin{pmatrix} \boldsymbol{U}_0 \\ \boldsymbol{U}_{01} \end{pmatrix} = \begin{bmatrix} \boldsymbol{G}_{11}^0 & \boldsymbol{G}_{12}^0 \\ \boldsymbol{G}_{21}^0 & \boldsymbol{G}_{22}^0 \end{bmatrix} \begin{pmatrix} \boldsymbol{T}_0 \\ \boldsymbol{T}_{01} \end{pmatrix} + \begin{pmatrix} \boldsymbol{u}_0^{(in)} \\ \boldsymbol{u}_{01}^{(in)} \end{pmatrix} \tag{0}$$

where,

$\boldsymbol{U}_0, \boldsymbol{T}_0$: Displacement and traction vectors on the boundary Γ_0,

$\boldsymbol{U}_{01}, \boldsymbol{T}_{01}$: Displacement and traction vectors on the boundary Γ_{01},

$\boldsymbol{H}_{ij}^0, \boldsymbol{G}_{ij}^0$: Coefficient matrices containing the contributions of the surface integrals of the Green's functions of traction and displacement of the region V_0,

$\boldsymbol{u}_0^{(in)}, \boldsymbol{u}_{01}^{(in)}$: Seismic wave motion displacements on the boundaries Γ_0 and Γ_{01},

in which $\boldsymbol{u}_0^{(in)}, \boldsymbol{u}_{01}^{(in)}$ are evaluated by the seismic waves radiated from the kinematic source model in a full space (for example, the explicit equations can be seen in the paper Harada, et al.[5]).

Similarly, denoting the notations for the region V_1 as follows,

$\boldsymbol{U}_1, \boldsymbol{T}_1$: Displacement and traction vectors on the boundary Γ_1,

$\boldsymbol{H}_{ij}^1, \boldsymbol{G}_{ij}^1$: Coefficient matrices containing the contributions of the surface integrals of the Green's functions of traction and displacement of the region V_1,

we obtain the following matrix form of boundary integral equation of the interior problems, for the region V_1,

$$\begin{bmatrix} \boldsymbol{H}_{11}^1 & \boldsymbol{H}_{12}^1 \\ \boldsymbol{H}_{21}^1 & \boldsymbol{H}_{22}^1 \end{bmatrix} \begin{pmatrix} \boldsymbol{U}_1 \\ \boldsymbol{U}_{01} \end{pmatrix} = \begin{bmatrix} \boldsymbol{G}_{11}^1 & \boldsymbol{G}_{12}^1 \\ \boldsymbol{G}_{21}^1 & \boldsymbol{G}_{22}^1 \end{bmatrix} \begin{pmatrix} \boldsymbol{T}_1 \\ -\boldsymbol{T}_{01} \end{pmatrix} \tag{2}$$

in which, $-\boldsymbol{T}_{01}$ stand for the inverse direction of the traction $\boldsymbol{T}_{01}$ of the region V_0.

Now, noting that the unknown displacement and traction vectors in the above eqs. (1) and (2) are $\boldsymbol{U}_0, \boldsymbol{U}_{01}, \boldsymbol{U}_1, \boldsymbol{T}_{01}$, and the tractions $\boldsymbol{T}_0, \boldsymbol{T}_1$ on the free ground surface are known as zero, and then combining eq. (1) with eq.(2), the following matrix equation can be derived for the entire system of Fig. 1,

$$\begin{bmatrix} \boldsymbol{H}_{11}^0 & \boldsymbol{H}_{12}^0 & -\boldsymbol{G}_{12}^0 & \boldsymbol{0} \\ \boldsymbol{H}_{21}^0 & \boldsymbol{H}_{22}^0 & -\boldsymbol{G}_{22}^0 & \boldsymbol{0} \\ \boldsymbol{0} & \boldsymbol{H}_{12}^1 & \boldsymbol{G}_{12}^1 & \boldsymbol{H}_{11}^1 \\ \boldsymbol{0} & \boldsymbol{H}_{22}^1 & \boldsymbol{G}_{22}^1 & \boldsymbol{H}_{21}^1 \end{bmatrix} \begin{pmatrix} \boldsymbol{U}_0 \\ \boldsymbol{U}_{01} \\ \boldsymbol{T}_{01} \\ \boldsymbol{U}_1 \end{pmatrix} = \begin{bmatrix} \boldsymbol{G}_{11}^0 & \boldsymbol{0} \\ \boldsymbol{G}_{21}^0 & \boldsymbol{0} \\ \boldsymbol{0} & \boldsymbol{G}_{11}^1 \\ \boldsymbol{0} & \boldsymbol{G}_{21}^1 \end{bmatrix} \begin{pmatrix} \boldsymbol{T}_0 \\ \boldsymbol{T}_1 \end{pmatrix} + \begin{pmatrix} \boldsymbol{u}_0^{(in)} \\ \boldsymbol{u}_{01}^{(in)} \\ \boldsymbol{0} \\ \boldsymbol{0} \end{pmatrix} \tag{3}$$

Finally, the unknown displacement and traction vectors $\boldsymbol{U}_0, \boldsymbol{U}_{01}, \boldsymbol{U}_1, \boldsymbol{T}_{01}$ on the boundaries can be obtained by solving the linear equation (3) in matrix form. Equation.(3) is the final form and usually used in the analysis of the entire system as shown in Fig.1. Assuming that the surface of the boundaries are divided into N_0 elements for the boundary Γ_0, N_{01} for the boundary Γ_{01}, and N_1 for the boundary Γ_1, by the so called constant elements, the number of unknown parameters is $3(N_0 + 2N_{01} + N_1)$ in eq.(3) since the displacement and traction vectors in each constant element have 3 components. In solving the linear eq. (3), we need the big capacity of computational memory and the long computational time, in such a case as to simulate earthquake ground motions of the entire system consisting of an earthquake source and the laterally inhomogeneous sedimentary layer as shown in Fig. 1.

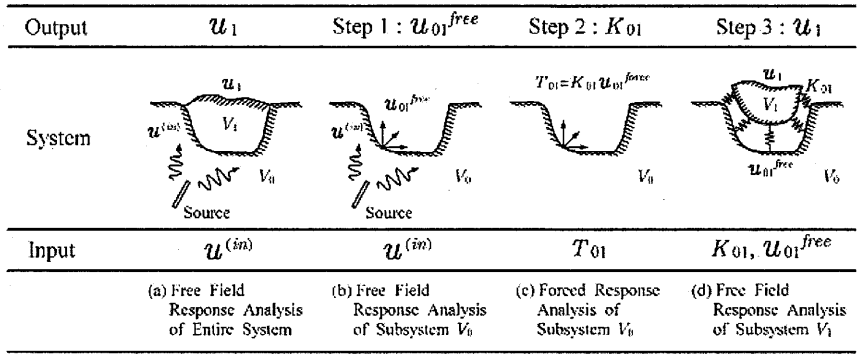

Figure 2 Schematical explanation of a method of subsystems analysis

FORMULATION OF SUBSYSTEMS ANALYSIS USING BEM

We start from a schematical explanation, showing the physical meanings as shown in Fig. 2, of a method of subsystems analysis developed in this paper. For simplicity of explanation of the subsystems analysis, we describe the method using the case where the entire system consisting of an earthquake source and the sedimentary layer is divided into two subsystems or regions V_0 and V_1. In this case, the free field ground motions of the entire system can be obtained from the following three steps:

(1) Computation of free field ground motions of the subsystem without sedimentary surface layer as shown in Fig.2 (b),
(2) Computation of stiffness matrices of the subsystem without earthquake source and sedimentary surface layer as shown in Fig.2 (c),
(3) Computation of free field ground motions of the sedimentary surface layer with use of the stiffness matrices of the step (2) and the free field motions of step (1) as shown in Fig. 2 (d).

We will show the corresponding formulations to the above physically significant descriptions in each step in the followings.

In the above step (1), the traction vectors $\boldsymbol{T}_0$, $\boldsymbol{T}_1$ on the free field ground surface are equal to zero in eq.(1), and then the free field ground motions $\boldsymbol{u}_0^{free}$, $\boldsymbol{u}_{01}^{free}$ can be obtained by solving the linear equation as

$$\begin{bmatrix} \boldsymbol{H}_{11}^0 & \boldsymbol{H}_{12}^0 \\ \boldsymbol{H}_{21}^0 & \boldsymbol{H}_{22}^0 \end{bmatrix} \begin{pmatrix} \boldsymbol{U}_0^{free} \\ \boldsymbol{U}_{01}^{free} \end{pmatrix} = \begin{pmatrix} \boldsymbol{u}_0^{(in)} \\ \boldsymbol{u}_{01}^{(in)} \end{pmatrix} \tag{4}$$

Also, in the above step (2), the input seismic wave motions $\boldsymbol{u}_0^{(in)}$, $\boldsymbol{u}_{01}^{(in)}$ are zero and the traction $\boldsymbol{T}_0$ also zero in eq.(1), and then the displacement vectors $\boldsymbol{U}_0^{force}$, $\boldsymbol{U}_{01}^{force}$ on the free surface due to the traction $\boldsymbol{T}_{01}$ can be obtained from the linear equation as follows,

$$\begin{bmatrix} \boldsymbol{H}_{11}^0 & \boldsymbol{H}_{12}^0 \\ \boldsymbol{H}_{21}^0 & \boldsymbol{H}_{22}^0 \end{bmatrix} \begin{pmatrix} \boldsymbol{U}_0^{force} \\ \boldsymbol{U}_{01}^{force} \end{pmatrix} = \begin{bmatrix} \boldsymbol{G}_{11}^0 & \boldsymbol{G}_{12}^0 \\ \boldsymbol{G}_{21}^0 & \boldsymbol{G}_{22}^0 \end{bmatrix} \begin{pmatrix} \boldsymbol{0} \\ \boldsymbol{T}_{01} \end{pmatrix} \tag{5}$$

From eq. (5), the traction $\boldsymbol{T}_{01}$ can be expressed as

$$\boldsymbol{T}_{01} = \boldsymbol{K}_{01}\boldsymbol{U}_{01}^{force} \tag{6.a}$$

where $\boldsymbol{K}_{01}$ may be called as the stiffness matrix or the complex spring depending on frequency,

$$\boldsymbol{K}_{01} = \left[\boldsymbol{H}_{21}^{0}\left(\boldsymbol{H}_{11}^{0}\right)^{-1}\boldsymbol{G}_{12}^{0} - \boldsymbol{G}_{22}^{0}\right]^{-1}\left[\boldsymbol{H}_{21}^{0}\left(\boldsymbol{H}_{11}^{0}\right)^{-1}\boldsymbol{H}_{12}^{0} - \boldsymbol{H}_{22}^{0}\right] \tag{6.b}$$

Now, considering the following compatibility condition of the displacement vectors of the entire system and the subsystems,

$$\begin{pmatrix}\boldsymbol{U}_{0}\\ \boldsymbol{U}_{01}\end{pmatrix} = \begin{pmatrix}\boldsymbol{U}_{0}^{free} + \boldsymbol{U}_{0}^{force}\\ \boldsymbol{U}_{01}^{free} + \boldsymbol{U}_{01}^{force}\end{pmatrix} \tag{7}$$

the traction $\boldsymbol{T}_{01}$ in eq.(6a) can be written as

$$\boldsymbol{T}_{01} = \boldsymbol{K}_{01}\boldsymbol{U}_{01}^{force} = \boldsymbol{K}_{01}\left(\boldsymbol{U}_{01} - \boldsymbol{U}_{01}^{free}\right) \tag{8}$$

Substituting eq.(8) into eq.(2), we can derive the following equation,

$$\begin{bmatrix}\boldsymbol{H}_{11}^{1} & \boldsymbol{H}_{12}^{1} + \boldsymbol{G}_{12}^{1}\boldsymbol{K}_{01}\\ \boldsymbol{H}_{21}^{1} & \boldsymbol{H}_{22}^{1} + \boldsymbol{G}_{22}^{1}\boldsymbol{K}_{01}\end{bmatrix}\begin{pmatrix}\boldsymbol{U}_{1}\\ \boldsymbol{U}_{01}\end{pmatrix} = \begin{bmatrix}\boldsymbol{G}_{11}^{1} & \boldsymbol{G}_{12}^{1}\\ \boldsymbol{G}_{21}^{1} & \boldsymbol{G}_{22}^{1}\end{bmatrix}\begin{pmatrix}\boldsymbol{T}_{1}\\ \boldsymbol{K}_{01}\boldsymbol{U}_{01}^{free}\end{pmatrix} \tag{9}$$

Equation.(9) is the system equation of the step (3) for the subsystem shown in Fig. 2 (d).

Finally, we can obtain the unknown displacement vector $\boldsymbol{U}_{0}$ from the following equation which is derived by arranging eq. (1) so as to write the unknown vectors in the left hand side,

$$\begin{bmatrix}\boldsymbol{H}_{11}^{0} & -\boldsymbol{G}_{12}^{0}\\ \boldsymbol{H}_{21}^{0} & -\boldsymbol{G}_{22}^{0}\end{bmatrix}\begin{pmatrix}\boldsymbol{U}_{0}\\ \boldsymbol{T}_{01}\end{pmatrix} = -\begin{bmatrix}\boldsymbol{H}_{12}^{0}\\ \boldsymbol{H}_{22}^{0}\end{bmatrix}\boldsymbol{U}_{01} + \begin{pmatrix}\boldsymbol{u}_{0}^{(in)}\\ \boldsymbol{u}_{01}^{(in)}\end{pmatrix} \tag{10}$$

At now, we call the analysis based on eqs. (9) and (10), where the rigorous stiffness matrix $\boldsymbol{K}_{01}$ obtained from eq.(6) is used, as the rigorous subsystems analysis. On the other hand, we call the same analysis, but where the approximate stiffness matrix instead of the rigorous stiffness matrix is used, as the approximate subsystems analysis. The approximate stiffness matrix is given by the analytical form using the so called dashpot modellings usually used as the approximate representation of the half space, because, for the high frequency range, the wavefronts due to the traction $\boldsymbol{T}_{01}$ in the subsystem shown in Fig. 2 (c) (step (2)) may tend to lie normal to the wavefront.

Now, we summarize the number of unknown parameters for the subsystems analysis: in the step (1) represented by eq. (4), the number of unknown parameters is $3(N_0 + N_{01})$, in the step (2) represented by eq.(6), $3N_{01}$, in the step (3) solving eq.(9), $3(N_{01} + N_1)$, and in the step (3) solving eq.(10), $3(N_0 + N_{01})$.

It is evident that the number of unknown parameters in the rigorous subsystems analysis is less than $3(N_0 + N_{01})$ or $3(N_{01} + N_1)$. Therefore, comparing with the number of unknowns $3(N_0 + 2N_{01} + N_1)$ in the entire analysis, the subsystems analysis is expected to require the less capacity of computational memory and the shorter computational time. The approximate subsystems analysis may be excellent in the capacity of computational memory and the computational time, since it does not need the matrix multiplication including the inverse transformation of the matrix. Comparison of the required capacity of the computational memory and the computational time will be described in the next section using a numerical example.

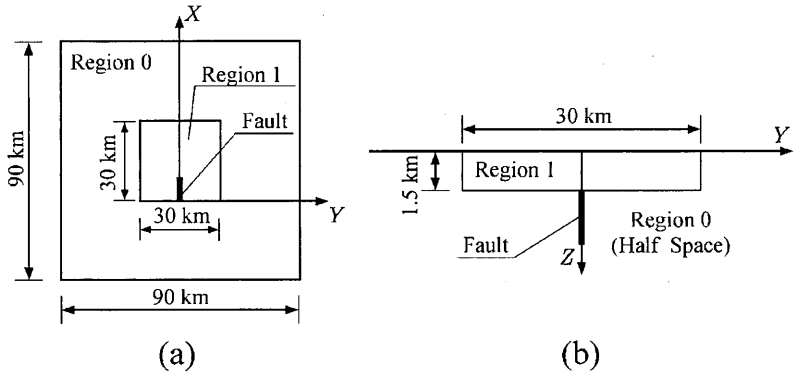

Figure 3 Strike slip fault and sedimentary rectangular valley used in numerical example

Table 1 Material properties of valley and bedrock used in numerical example

	P wave Speed [m/s]	S wave Speed [m/s]	Density ρ [t/m^3]	Damping Ratio
Region 0	6000	3500	2.8	0.00125
Region 1	2800	1600	2.3	0.00333

NUMERICAL EXAMPLES OF SEISMIC WAVE MOTIONS

Model Description of Sedimentary Valley and Fault Rupture

In order to verify the formulations of the rigorous and approximate subsystems analyses presented in the previous section, and to examine their performance in the capacity of computational memory and the computational time, we simulate the earthquake ground motions using the methods of entire system analysis, rigorous subsystems analysis and approximate subsystems analysis, and then we compare the simulated ground motions, and discuss the accuracy and advantage of the proposed methods of subsystems analysis.

We use an idealized rectangular sedimentary valley as shown in Fig. 3 in the simulation of ground motions. We assume that a strike slip fault rupture occurs at the bedrock underneath the central portion of the valley. The material properties of the sedimentary valley and the bedrock are shown in Table 1.

The surface of the boundary of the rectangular sedimentary valley is discretized by the quadrilateral constant elements with 1.5km by 1.5km size, while the surface of the boundary of the bedrock is divided by the quadrilateral constant elements with 3.0km by 3.0km size. Therefore the number of elements are N_0 =800, N_{01}=480, and N_1=400 in this numerical example. By considering the material properties of the sedimentary valley and the size of the elements, the wave motions up to the frequency 2.0 rad/s are analysed in this numerical example.

The assumed strike slip fault rupture is shown in Fig. 4. The length and the width of the fault are 8.5km and 8.5km. The adopted fault rupture in this numerical example is cited from the studies of Bouchon [4], Harada et al.[5]. The rupture starts from the left side of the fault with the constant speed of 2.2km/s to the right direction. The source parameters of the extended fault rupture are indicated in Table 2.

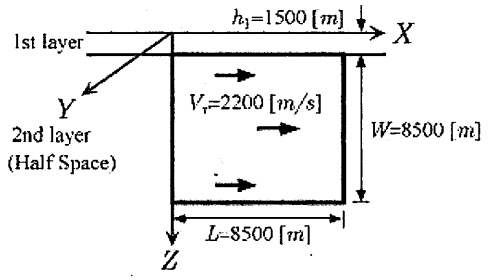

Figure 4 Model of a strike slip fault rupture used in numerical example

Table 2 Parameter of strike slip fault rupture used in numerical example

Seismic Moment M_0	[N·m] ([dyne·cm]	2.230×10^{17} 2.230×10^{24})
Rize Time τ	[sec]	0.3
Length L	[m]	8500
Width W	[m]	8500
Rupture Speed v_r	[m/sec]	2200
Depth of Fault z_{so}	[m]	0.0
Strike Angle ϕ	[°]	0.0
Dip Angle δ	[°]	90.0
Slip Angle λ	[°]	0.0
Slip Type		Type 1

Frequency Response of Valley Due to Plane SH wave

Herein, we compare the frequency response functions of the free field surface of rectangular sedimentary valley due to the vertically incident plane SH wave. Figure 5 shows the spatial variation of frequency response functions along the x axis, which crosses the centre of the valley, for five frequencies, $\omega =$ 0.0625, 0.5, 1.0, 1.5, 2.0 rad/s. The spatial variation of the frequency response functions shown in Fig. 5 are computed using the method of entire system analysis (indicated by the curves in Fig. 5) and the method of rigorous subsystems analysis (indicated by the symbols in Fig. 5), while the same spatial variation of the frequency response functions computed by the method of entire system analysis (indicated by the curves in Fig. 6) and the method of approximate subsystems analysis (indicated by the symbols in Fig. 6) are shown in Fig. 6.

From Fig. 5, we observe the perfect coincidence of the frequency response functions, indicating the rigorous subsystems analysis presented in this paper is valid. Also we observe from Fig. 6 that the approximate subsystems analysis can compute the very similar frequency response functions to those from the method of entire system analysis.

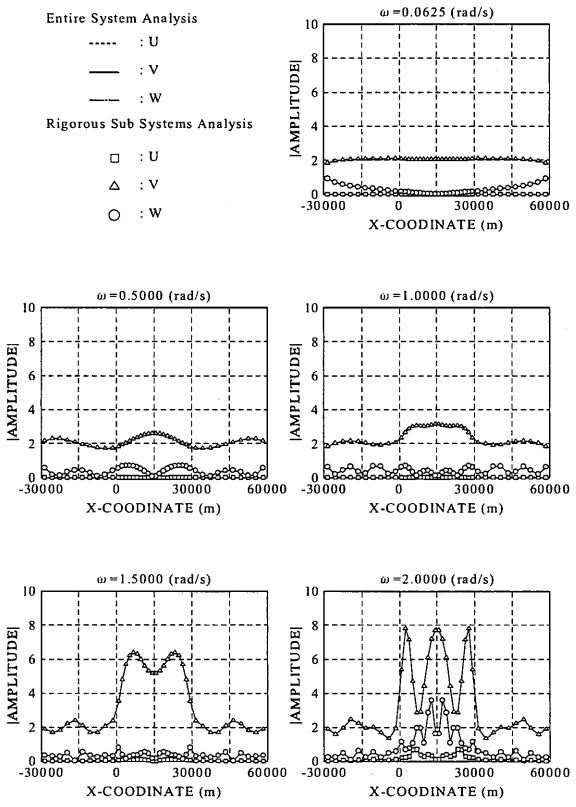

Figure 5 Spatial variation of frequency response functions due to SH wave (Curves; Entire system analysis, and Symbols; rigorous subsystem analysis)

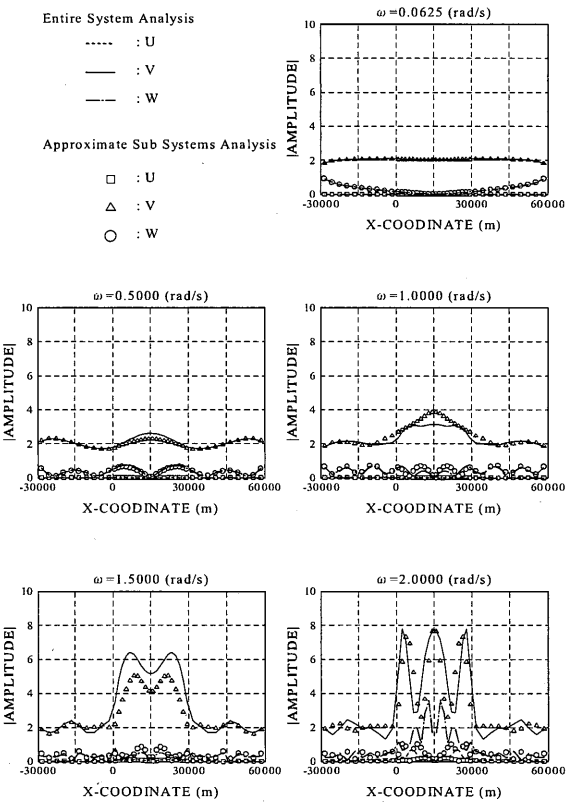

Figure 6 Spatial variation of frequency response functions due to SH wave (Curves; Entire system analysis, and Symbols; Approximate subsystem analysis)

Free Field Ground Motions of Sedimentary Valley Due to Fault Rupture

Herein we compare the time histories of ground motion velocity at 4 points on the free surface of the sedimentary valley due to the fault rupture. Figure 7 shows the fault normal components of the time histories of ground motion velocity at 4 points. They are obtained by the method of entire system analysis (indicated by the solid curves in Fig. 7) and the method of rigorous subsystems analysis (indicated by the broken curves in Fig. 7). On the other hand, the time histories of ground motion velocity computed by the method of entire system analysis (indicated by the solid curves in Fig. 8), and the method of approximate subsystems analysis (indicated by the broken curves in Fig. 8), are shown in Fig. 8.

From Fig. 7, we observe the perfect coincidence of the time histories of ground motion, indicating the rigorous subsystems analysis presented in this paper is valid. Also we observe from Fig. 8 that the approximate subsystems analysis can simulate the very similar time histories to those from the method of entire system analysis.

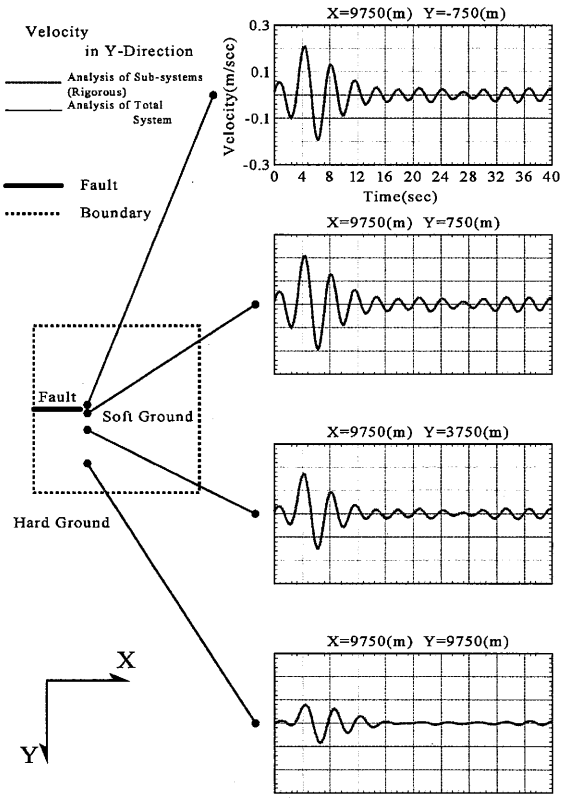

Figure 7 Fault normal component of ground motion velocity time histories (Solid curves; Entire system analysis, and Broken curves; Rigorous subsystem analysis)

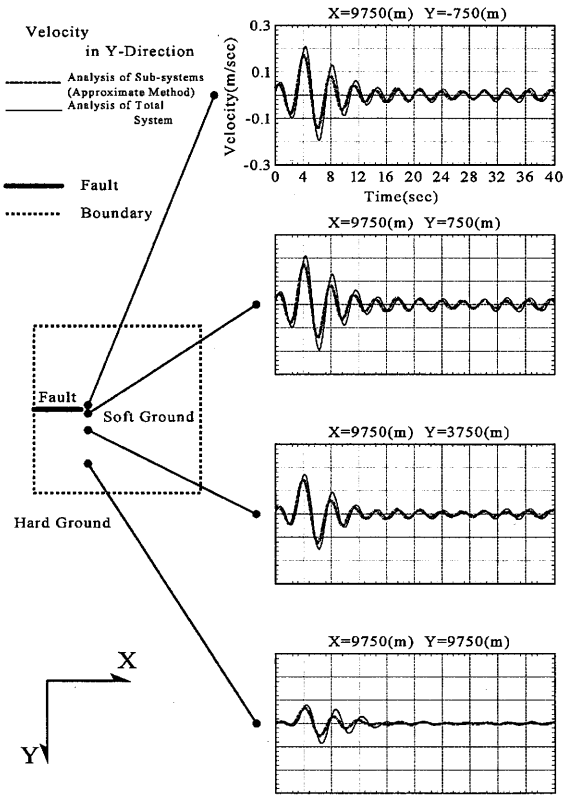

Figure 8 Fault normal component of ground motion velocity time histories (Solid curves; Entire system analysis, and Broken curves Approximate subsystem analysis)

NUMERICAL ADVANTAGES OF SUBSYSTEMS ANALYSIS

Finally, we compare the capacity of computational memory and the computing time required in the computation of responses of sedimentary valley. In this comparison, the maximum required memories and the computational time, in the computation of the frequency responses of the valley for a certain frequency in the case of the simulation of ground motions in the previous sections (Figs. 7 and 8), are depicted and indicated in Table 3. Of course, the values of the required capacity of computational memory and the computational time in Table 3 depend on the computer and the computer code used in the simulation, but they indicate the relative numerical advantages of the subsystems analyses if we compare these values among the used methods for computation.

We can observe from Table 3 that the methods of rigorous subsystems analysis and approximate subsystems analysis require only about a half, and a quarter of the capacity of computational memory necessary for the method of entire system analysis. Concerning the computational times indicated in table 3, there is nothing to choose between the rigorous subsystems analysis and the entire system analysis, but the approximate subsystems analysis is superior among the 3 methods.

By the way, in the engineering simulation of ground motions, the following two parametric studies may be performed to investigate the effect of uncertainties on the simulated ground motions; (1) Investigation of the effect of the surface topography and the material properties of the sedimentary valley on the ground motions, and (2) Investigation of the effect of earthquake source parameters on the ground motions. For these parametric studies the subsystems analysis, especially the method of approximate subsystems analysis, may exhibit its power to the full, because it requires the parametric studies for only one subsystem.

Table 3 Comparison of the maximum memories and computational times

	Entire system analysis	Rigorous sub systems analysis	Approximate sub systems analysis
Number of elements	$N_0+2N_{01}+N_1$ 2160	N_0+N_{01} 1280	N_0+N_{01} 1280
Maximum memories	About 1,338Mbyte	About 609MByte	About 365Mbyte
Computation times	About 30 minutes	About 40 minutes	About 25 minutes

CONCLUSIONS

In this paper, in order to improve the required capacity of computational memory and the computational time, which are the week points of the 3 dimensional direct boundary element method when it is used in the simulation of ground motions for the entire system consisting of an earthquake source and the inhomogeneous layered media, the method of subsystems analysis with making use of the direct boundary element method has been developed. The advantages of the developed method of subsystems analysis have been demonstrated by the numerical examples of the simulation of ground motions of the sedimentary valley due to an earthquake source, by indicating the results of drastic reduction of requiring computer memory and computational time.

The method of subsystems analysis developed in this paper has the following three step computations when the entire system of earthquake source and inhomogeneous sedimentary layered media is divided

into two subsystems; the earthquake source and earthcrust system, and the sedimentary surface layer system.

(1) Computation of free field ground motions for the fault and earthcrust system without the sedimentary surface layer system,
(2) Computation of stiffness matrices for the earthcrust system without fault and sedimentary surface layer system,
(3) Computation of free field ground motions for the sedimentary surface layer system with use of the stiffness matrices of the step (2) and the free field motions of step (1).

The method of subsystems analysis presented in this paper can be extended to the method of multiple subsystems analysis.

REFFERENCES

1. Pao, Y-H, and Varatharajulu, V. "Huygens' principle, radiation conditions, and integral formilas for the scattering of elastic waves." Journal of Acoustic Society of America, 1976;Vol.59, No.6, 1361-1371.
2. Aki,K. and Richards,P.G. "Quantitative Seismology,Theory and Methods.", W.H.Freeman and Company,1980.
3. Manolis,G.D., and Beskos,D.E. "Boundary Element Methods in Elastodynamics.", Unwin Hyman Publication,1988
4. Bouchon, M. "Predictability of ground displacement and velocity near an earthquake fault, an example: The Parkfield Earthquake of 1966." Journal of Geophysical Research, 1979; Vol. 84, No.B11, pp.6149-6156.
5. Harada,T. ,Ohsumi,T., and Okukura,H. "Analytical solutions of wave field in 3-D Cartesian coordinate and their application to synthesis of seismic ground motions", Journal of Japan Society of Civil Engineers, 1999; No.612/I-46, pp.99-108 (in Japanese).